

SACRAMENTO RIVER FLOW RECONSTRUCTED TO A.D. 869 FROM TREE RINGS¹

David M. Meko, Matthew D. Therrell, Christopher H. Baisan, and Malcolm K. Hughes²

ABSTRACT: A time series of annual flow of the Sacramento River, California, is reconstructed to A.D. 869 from tree rings for a long-term perspective on hydrologic drought. Reconstructions derived by principal components regression of flow on time-varying subsets of tree-ring chronologies account for 64 to 81 percent of the flow variance in the 1906 to 1977 calibration period. A Monte Carlo analysis of reconstructed n -year running means indicates that the gaged record contains examples of drought extremes for averaging periods of perhaps = 6 to 10 years, but not for longer and shorter averaging periods. For example, the estimated probability approaches 1.0 that the flow in A.D. 1580 was lower than the lowest single-year gaged flow. The tree-ring record also suggests that persistently high or low flows over 50-year periods characterize some parts of the long-term flow history. The results should contribute to sensible water resources planning for the Sacramento Basin and to the methodology of incorporating tree-ring data in the assessment of the probability of hydrologic drought.

(KEY TERMS: drought; modeling; meteorology/climatology; dendrohydrology; Sacramento River.)

INTRODUCTION

The Sacramento River is a vital source of surface water for California. The 69,000 km² watershed includes much of northern California, and the outflow to San Francisco Bay makes up more than 30 percent of the flow of all rivers in the state (Crippen, 1986). Water resources planning for the Sacramento River requires information on the variability of runoff imposed by climate. As with many basins in the western United States, the likelihood of severe hydrologic drought is of particular interest. Lacking reliable predictions of climatic departures even a season in

advance, we must rely on the gaged flow record for estimates of this likelihood. But the gaged record cannot be expected to represent low-frequency fluctuations or periodic shifts in runoff that might be caused by changing climatic regimes, or to contain all critical low-flow events important to planners.

Tree-ring analysis has been used to extend time series for assessing the variability of river flow beyond the gaged record (e.g., Smith and Stockton, 1981; Cook and Jacoby, 1983; Cleaveland and Stahle, 1989; Meko and Graybill, 1995). The useful extension is limited only by the length of climatically sensitive tree-ring chronologies in or near the basin. In an earlier tree-ring study of the Sacramento Basin, regression models with tree-ring indices as predictors were found to account for more than 50 percent of the variance of annual flow at some gages (Earle and Fritts, 1986). The 1930s comprised the single longest period of reduced flows in reconstructions to A.D. 1560; verification statistics were weak, however, and the reconstructions relied heavily on the climate signal from a single tree-ring chronology outside the basin.

In this paper we describe results of a new Sacramento River reconstruction from a network of tree-ring sites with time coverage extended back to A.D. 869 and spatial coverage of the basin greatly improved after A.D. 1630. We apply a Monte Carlo analysis to incorporate the reconstruction uncertainty into a comparison of reconstructed and actual hydrologic droughts as summarized by n -year running means of annual flow.

¹Paper No. 00106 of the *Journal of the American Water Resources Association*. Discussions are open until April 1, 2002.

²Respectively, Research Specialist, Laboratory of Tree-Ring Research, University of Arizona, Tucson, Arizona 85721; University of Arkansas Tree-Ring Laboratory, Department of Geoscience, 113 Ozark Hall, Fayetteville, Arkansas 72701; and Research Specialist and Professor of Dendrochronology, Laboratory of Tree-Ring Research, University of Arizona, Tucson, Arizona 85721 (E-Mail/Meko: dmeko@LTRR.arizona.edu).

DATA

Streamflow data, tree-ring data, and precipitation data were used in the study. The streamflow series is the unimpaired annual (water-year) flow record for the Sacramento River. This series, downloaded from the Worldwide Web (California Department of Water Resources, 2000), is the sum of four components: (1) the Sacramento River above the gage at Bend Bridge, (2) the inflow of the Feather River to Lake Oroville, (3) the Yuba River at Smartville, and (4) the inflow of the American River to Folsom Lake (Figure 1). The unimpaired water-year-total flow series, referred to from here on as "flow," is an estimate of the natural river flow of the basin, or the flow with the effects of development removed. The flow series covers the period 1906 to 1999, has a long-term mean of 18.1 MAF, and ranges from 5.12 MAF to 37.65 MAF.

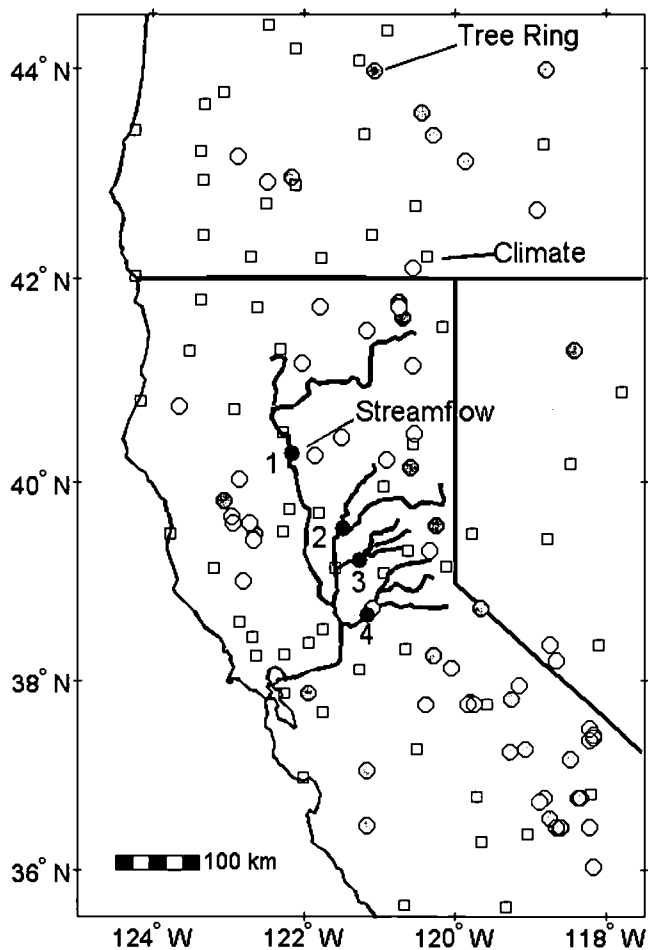


Figure 1. Locations of Tree-Ring Sites, Precipitation Stations, and Stream Gages. The 36 tree-ring sites selected in the precipitation screening are denoted by shaded circles and the 35 eliminated sites by open circles. The four numbered black dots denote gages or stream reference locations described in the text.

The tree-ring data are standard chronologies of ring-width indices (Fritts, 1976) for 71 tree-ring sites in northern California and surrounding areas (Figure 1). The chronologies were downloaded from the International Tree-Ring Data Bank (NGDC, 2000), developed from our own collections, and obtained by personal communication with other dendrochronologists. All chronologies from 35.5° to 44.5°N latitude and 117.5° to 125°W longitude with time coverage A.D. 1700 to 1961 were included in the initial network (Figure 1). Monthly precipitation data for 70 United States Historical Climate Network (USHCN) stations in this same area were downloaded from the Web (NCDC, 2000).

METHODS

Screening and Filtering of Tree-Ring Chronologies

Tree-ring chronologies unrelated to water-year-total precipitation were eliminated from the study by screening chronologies with precipitation data using multiple linear regression (MLR). Precipitation data were first interpolated to the tree-ring sites by inverse-distance weighting of standardized monthly station precipitation anomalies (Jones and Hulme, 1996). Water-year-total precipitation at a site was then regressed against the site chronology in a distributed lag regression model, using the tree-ring chronology in years t , $t + 1$, and $t + 2$ as the predictors of precipitation in year t . Chronologies with regression $R^2 < 0.10$, corresponding roughly to marginal significance ($\alpha = 0.05$) of the overall- F for regression (Weisberg, 1985), were dropped from the analysis. Screening reduced the tree-ring network from 71 chronologies to 36 chronologies, all covering the years A.D. 1630 to 1977 (Figure 1). Remaining chronologies were classified as having strong ($R^2 > 0.33$), moderate ($0.25 < R^2 \leq 0.33$), or weak ($0.10 < R^2 \leq 0.25$) precipitation signal. The 0.33 and 0.25 thresholds are roughly the 75th and 50th percentiles of R^2 values for the 36 chronologies. Site information, including the computed R^2 from precipitation screening, is included in the Appendix.

Exploratory data analysis indicated that the tree-ring chronologies were more highly autocorrelated than the flow series for the common period 1906 to 1977: the first-order autocorrelation coefficient is 0.11 for flow, but exceeds 0.33 for most chronologies, and is higher than 0.70 for several. The elevated autocorrelation in tree-ring data is an artifact of biological processes (e.g., food storage, multi-year needle retention, root and crown dieback) and is a source of noise

in the modeling of flow on tree-ring indices. We adjusted the full-length chronologies for autocorrelation by filtering them with a simple lag-one filter

$$x_t = w_t - cw_{t-1} \quad (1)$$

where w_t is the departure of the tree-ring index in year t from its long-term mean, x_t is the filtered index, and c is the filter coefficient such that the 1906 to 1977 segment of x_t has a first-order autocorrelation of approximately 0.11. The value for c was estimated by trial-and-error, iteratively incrementing c in steps of 0.01 over the interval {0,1}.

Reconstruction Modeling

Reconstruction equations were estimated by regressing \log_{10} flow on principal components (PCs) of tree-ring indices. Log-transformation was necessary to adjust for heteroscedasticity in the relationship between flow and tree rings – a feature clearly visible as increased scatter at higher flows in plots of flow against tree-ring indices. The reconstruction model is given by

$$\hat{y} = \mathbf{X}\hat{\mathbf{b}} \quad (2)$$

where \mathbf{X} is a time series matrix of a subset of the tree-ring PCs, $\hat{\mathbf{b}}$ is a vector of estimated regression coefficients, and \hat{y} is a vector time series of reconstructed \log_{10} flows. Mathematical details of principal components regression (PCR) can be found in Mardia *et al.* (1979). Application of PCR and related orthogonal spatial regression models to climate reconstruction from tree rings is described by Cook *et al.* (1994).

Separate models of the form (Equation 2) were developed for three subperiods of the tree-ring record: A.D. 869 to 1099, A.D. 1100 to 1629, and A.D. 1630 to 1977. Reconstruction by subperiods allowed us to take advantage of the improving site coverage of the basin with time while not sacrificing length of reconstruction. For a subperiod, the first step was to convert the tree-ring indices to orthogonal variables by principal components analysis (PCA) of the correlation matrix for the 1906 to 1977 calibration period. For N_T available tree-ring chronologies, this step yielded N_T PCs. The next step was to reduce the tree-ring data by discarding the PCs with the smallest eigenvalues. The remaining N_p PCs were then used as the pool of potential predictors for the regression model to predict \log_{10} flow. Of these, only a subset of N_f PCs were entered as predictors in the final model, depending on the percentage of flow variance accounted for.

A multiplicity of models is possible by the above procedure, depending on how many PCs are included

in the pool of potential predictors, and on the criterion for “importance” in allowing a PC to enter as a predictor in the regression (e.g., the critical α -level for a t -test on the coefficients). With increasing size of the pool of potential predictors also comes an increased risk of overfitting the model by conventional stepwise regression methods for variable selection (Rencher and Pun, 1980).

Consequently, we relied on validation accuracy, using the predicted residual sum of squares, or PRESS statistic (Weisberg, 1985), to identify the best combination of N_p and N_f for the final reconstruction models. Models were fit and cross-validated within two nested loops. The outer loop is over $N_p = 1, \dots, N_p^*$ PCs included in the pool of potential predictors, where N_p^* is the number of PCs needed to account for 90 percent of the tree-ring variance. The inner loop is over $N_f = 1, \dots, N_p$ PCs included as final predictors in the regression model. At each iteration a model was estimated and cross-validated (Michaelsen, 1987), and three validation statistics were computed. The first two are the PRESS statistic

$$\text{PRESS} = \sum_{i=1}^m \hat{e}_{(i)}^2 \quad (3)$$

and the root mean square error of cross-validation

$$\text{RMSE}_v = \sqrt{\text{PRESS} / m} \quad (4)$$

where m is the length of calibration period, and $\hat{e}_{(i)}$ is the prediction error for observation i from a model fit to the $m-1$ observations not including observation i . The model with the lowest RMSE_v was selected as the reconstruction model. The third statistic is the reduction-of-error, RE, which measures the skill of prediction relative to that of a “null” prediction consisting of the calibration-period mean of flow as the predicted value for each year of the validation period (Gordon, 1982). RE is given by $\text{RE} = 1 - (\text{PRESS}/D)$, where D is the sum-of-squares of departures of predicted values from the calibration-period mean. RE can be near zero or even negative for reconstructions no more accurate than the null prediction. The maximum possible value of RE is 1, corresponding to perfect prediction for the validation period.

Monte Carlo Drought Analysis

The n -year running mean was selected as the measure to summarize hydrologic drought. Because the reconstruction has an associated error, the drought properties of the reconstruction should be interpreted

in probabilistic terms. Theoretical confidence bands for n -year means of the reconstruction in original flow units (MAF) cannot be computed directly from the regression error variance because the predictand is a nonlinear transformation of flow. We, therefore, resorted to a Monte Carlo analysis to incorporate the reconstruction uncertainty into the assessment of hydrologic drought. The method is similar to that described by Touchan and Meko (1999), except that our reconstruction is done with subperiod models rather than a single regression model, and that we draw our noise samples from a distribution whose variance equals the cross-validation mean square error rather than the regression mean square error. Weisberg (1985) suggests that if a regression model is used for predictions, the cross-validation mean square is a "sensible" estimate of the prediction error variance.

Let \hat{y}_i be a column vector of the reconstructed \log_{10} flows for a subperiod i . A sample of the same length as \hat{y}_i was drawn from a random normal distribution with mean zero and variance equal to the cross-validation error variance of the subperiod model. This sample, defined as the noise as vector ϵ_i , was added to the reconstruction to get a noise-added reconstruction for the subperiod

$$\hat{u}_i = \hat{y}_i + \epsilon_i \quad (5)$$

Noise-added reconstruction segments computed in this way for the three subperiods were merged into a single noise-added reconstruction vector \hat{u} .

The above process was repeated 1,000 times, and the resulting 1,000 noise-added reconstructions stored as columns in a time series matrix \hat{U} . The elements of \hat{U} were back-transformed by exponentiation from \log_{10} to volume units and the columns converted to m -year running means. The empirical distribution

function of the 1,000 values in the rows of \hat{U} was then used to assign exceedance probabilities of m -year mean flow to each m -year period of the reconstruction. The 0.1 and 0.9 quantiles of the distribution are the empirical 80 percent confidence bands for the reconstructed values.

RESULTS

Reconstruction Modeling

Tree-ring networks for the three sub-period models are shown on the map in Figure 2. The plotting symbols code the strength of precipitation signal in each chronology as estimated by the screening analysis. The networks for T869 and T1100 are striking for their lack of sites in the watershed. For these models, the flow signal for the Sacramento Basin must come from the similarity of climatic fluctuations in the basin with those to the north and south. Only the northernmost site (Frederick Butte, Oregon) in the two networks has a strong precipitation signal. Many tree-ring chronologies in the area have start years between A.D. 1100 and A.D. 1630, leading to vastly improved site coverage for model T1630. This model includes all 36 screened tree-ring sites, including nine with a strong precipitation signal. The strongest signals belong to *Quercus douglasii* and *Q. lobata* chronologies collected in California in the late-1990s as part of a larger collection that has been successfully applied to reconstruction of salinity levels in San Francisco Bay (D. W. Stahle, M. D. Therrell, M. K. Cleaveland, D. R. Cayan, M. D. Dettinger, and N. Knowles, A Blue Oak Perspective on San Francisco Bay Salinity: 1604-1997, manuscript in preparation).

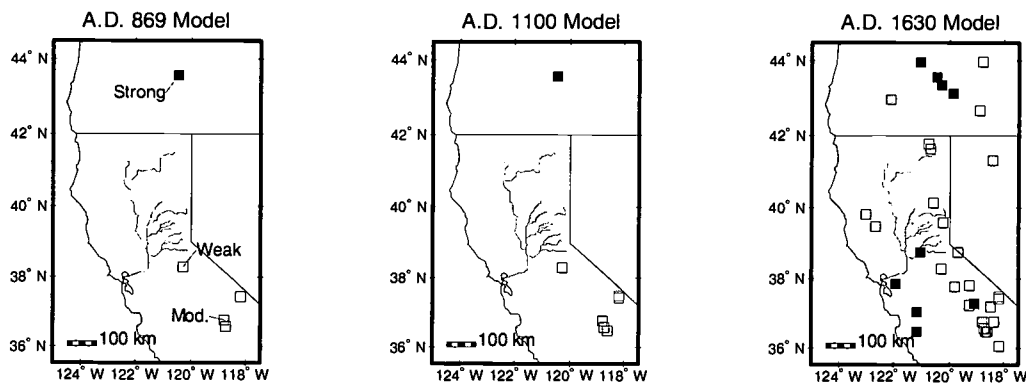


Figure 2. Map Showing Tree-Ring Networks for Subperiod Reconstruction Models. Shading indicates strength of precipitation signal in tree-ring chronology.

The number of tree-ring PCs used as predictors in the final sub-period reconstruction models ranges from three to nine (Table 1). The iterative fitting and cross-validating was substantially important in the reconstruction modeling only for model T1630, for which the nine predictors were culled from an initial network of 36 tree-ring sites. Ninety percent of the tree-ring variance in model T1630 was accounted for by the first 16 PCs. Cross-validation indicated no gain in predictive value for models more complicated than the selected $\{N_p = 12, N_f = 9\}$ model.

The accuracy of reconstruction increases with time for the subperiod models, presumably because of improving site coverage of the basin (Table 1). Regression R^2 ranges from 0.64 to 0.81. Cross-validation statistics indicate that these high R^2 values are not an artifact of overfitting: the reduction of error statistic (Gordon 1982) is large and positive, and the error of cross-validation is only slightly greater than that of calibration as measured by the root-mean-square errors (Table 1).

Analysis of regression residuals indicated no serious violations of regression assumptions. The null hypothesis that the residuals are normally distributed could not be rejected at the 0.01 α -level in a chi-square test of residuals (Conover, 1980). Scatter plots showed no discernible pattern of dependence of residuals on predicted values. Lagged scatter plots showed no evidence of time-dependence in residuals for model T1630, but some hint of positive dependence at a lag of one year for models T869 and T1100. The first-order autocorrelation coefficient is approximately 0.20 for the residuals from these earlier models, but is still small enough that the null hypothesis of zero first-order autocorrelation cannot be rejected at the 0.01 α -level in a Durbin-Watson test (Draper and Smith, 1981).

The high accuracy of the T869 and T1100 models ($R^2 \geq 0.64$) is surprising in the light of the sparseness

of the early tree-ring networks. Time series plots of actual and reconstructed \log_{10} flow for models T869 and T1630 show that T869 actually has smaller error than T1630 in a few scattered years (Figure 3). The value of the improved tree-ring coverage is evident, however, in the superior ability of T1630 to capture several features of the gaged flow poorly reconstructed by T869. Marked improvement is shown, for example, in the extreme low flows of 1976 and 1977, and in sequences of flows beginning in 1939 and 1952. Both models track year-to-year and multi-year fluctuations in flow reasonably well, including reversals from wet to dry conditions and vice versa.

Drought Analysis

The post-1629 reconstruction must be considered more reliable than the earlier reconstruction because of the superior regression statistics of model T1630 (Table 1) and the better spatial sampling of the watershed by the T1630 tree-ring network (Figure 2). The annual reconstructed series, back-transformed to volume units, is plotted in Figure 4, along with the gaged flow and a reference line at the single lowest gaged flow (5.12 MAF in 1977). No flow is reconstructed lower than the gaged flow for 1977, but the probability exceeds 0.10 that the flow was lower than 5.12 MAF in five reconstruction years: 1777, 1795, 1829, 1841, and 1864. These are the years for which the 80 percent confidence band around the reconstructed values overlaps the 1977 drought threshold (Figure 4).

For a perspective on drought in the post-1629 period, the ten lowest reconstructed and single lowest actual n -year running means for $n = 1, 3, 6, 10, 20,$ and 50 years are listed in Table 2. The 1930s dominate the drought listing for averaging periods of 6, 10 and 20 years and contain the lowest single-year

TABLE 1. Statistics of Reconstruction Models.

Model ^a	Period (A.D.) ^b	Number of Variables ^c			Model Statistics ^d			
		N_T	N_p	N_f	Calibration		Validation	
					R^2	RMSE _c	RE	RMSE _v
T869	869-1099	5	4	3	0.64	0.115	0.59	0.122
T1100	1100-1629	7	6	5	0.69	0.108	0.62	0.118
T1630	1630-1905	36	12	9	0.81	0.083	0.73	0.098

^aModel, labeled by starting year of subperiod.

^bStarting and ending years of reconstruction subperiods.

^cNumber of tree-ring sites (N_T), number of tree-ring PCs in pool of potential predictors (N_p), and number of PCs included as predictor variables in final reconstruction model (N_f).

^dRegression R^2 , root-mean-square error of calibration and cross-validation, and reduction-of-error statistic. Units of RMSE are \log_{10} million acre-ft.

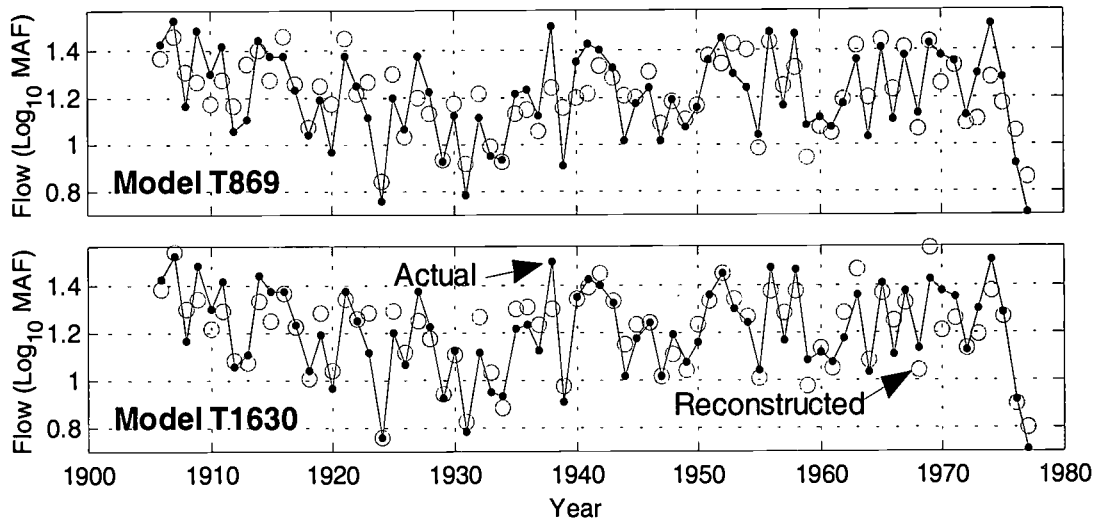


Figure 3. Time Series Plots Illustrating Agreement of Actual and Reconstructed Flows for Least Accurate and Most Accurate Subperiod Reconstruction Model. Regression R^2 is 0.64 for model T869 and 0.81 for model T1630.

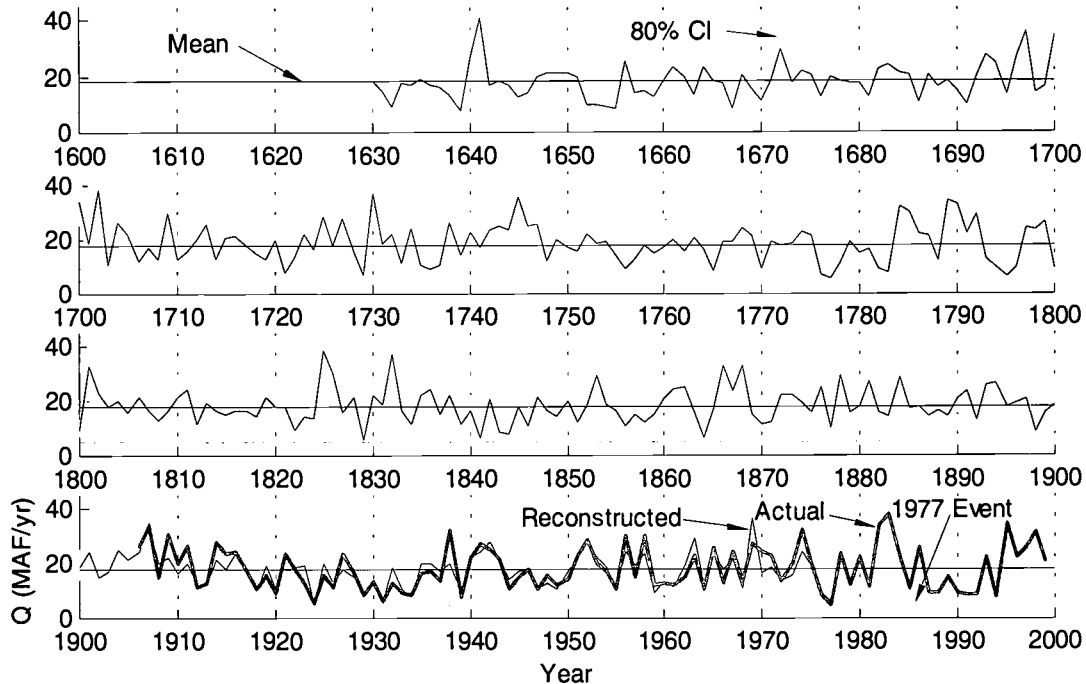


Figure 4. Time Series Plots of Gaged Annual Flow and Post-1629 Reconstruction. Uncertainty in reconstructed values shown by 80 percent confidence interval derived by Monte Carlo analysis. Reference lines at long-term 1906 to 1999 mean (18.1 MAF) and record low (5.12 MAF) of gaged flow. Upper confidence interval on high flows truncated to enhance readability.

reconstructed flow (1924) and fourth-lowest three-year mean (1929 to 1931). The period 1929 to 1934 is the lowest reconstructed six-year mean in the post-1630 reconstruction (Table 2). The 1990s, though outside the period of reconstruction, also stands out as an unusually severe long-term event. The time series

of gaged flow shows that the 1990s drought was similar in intensity and duration to the 1930s drought. Both droughts are characterized best by low flows over roughly a six-year period. The lowest gaged three-year mean occurred in 1990 to 1992; only two reconstructed three-year means were lower.

TABLE 2. Lowest n -Year Moving Averages of Reconstructed and Actual Flow in the Post-1629 Reconstruction.*

Rank	1 Year	3 Year	6 Year	10 Year	20 Year	50 Year
1	5.74(1924)	8.21(1778)	10.88(1934)	12.92(1933)	14.71(1936)	16.57(1961)
2	5.83(1829)	8.68(1796)	11.95(1844)	13.11(1934)	14.73(1939)	16.71(1962)
3	6.05(1777)	9.27(1655)	12.11(1846)	13.14(1935)	14.73(1937)	16.74(1960)
4	6.23(1864)	9.47(1931)	12.14(1933)	13.75(1931)	14.75(1934)	16.80(1959)
5	6.32(1977)	9.58(1795)	12.41(1931)	13.76(1783)	14.86(1935)	16.87(1964)
6	6.40(1795)	9.71(1654)	12.67(1781)	13.77(1932)	15.20(1931)	16.88(1966)
7	6.70(1931)	10.29(1737)	12.77(1935)	13.78(1848)	15.22(1938)	16.97(1957)
8	6.74(1841)	10.96(1977)	12.85(1657)	13.78(1846)	15.26(1858)	16.97(1967)
9	6.87(1776)	11.27(1783)	13.08(1782)	13.80(1937)	15.29(1940)	16.99(1965)
10	7.03(1729)	11.47(1841)	13.12(1845)	13.87(1936)	15.42(1941)	16.99(1968)
1	5.12(1977)	8.87(1992)	9.79(1934)	12.27(1937)	13.54(1937)	16.38(1966)

*Table entries are averages of water-year flow (MAF) for n -year period ending with year in parentheses; rows 1-10 are ten most severe reconstructed droughts and last row is most severe observed drought.

The full-length reconstruction, which starts in A.D. 869, indicates that extended periods of drought may have been more common before A.D. 1400 than after (Figure 5). The time series in Figure 5 have been smoothed with a six-year moving average to facilitate comparison of reconstructed droughts with those of the 1930s and 1990s. Similarly smoothed gaged flow is also plotted. The closeness of the curves for reconstructed and actual flow attests to the strong ability of the reconstruction to track interdecadal flow variations. The 1930s also emerges as an unusually severe drought in the context of the full-length reconstruction. Only two reconstructed six-year means, near A.D. 980, are lower than the reconstructed mean for 1929 to 1934. The severity of the 1930s drought in the Sierra Nevada in the context of the past 500 to 1000 years has been noted by other tree-ring researchers (Earle and Fritts, 1986; Graumlich, 1993; Graybill and Funkhouser, 2000). Given the uncertainty in the reconstruction, as shown by the Monte-Carlo-derived 80 percent confidence band in Figure 5, only four reconstructed six-year periods have a probability of at least 0.10 of being drier than 1929 to 1934: periods ending in A.D. 983, 984, 1301, and 1355.

The 20th Century is less representative of maximum drought severity for drought durations shorter and longer than six years. The five lowest reconstructed and single lowest gaged n -year means for $n = 1, 3, 6, 10, 20,$ and 50 years in the full-length reconstruction are listed in Table 3. Except for the six-year averaging period, none of the five lowest reconstructed means occurred in the 20th Century. Droughts ending near A.D. 1300 and A.D. 1400 dominate the listing of most severe droughts for averaging periods of ten years and longer. The lowest one-year and

three-year means occurred in 1580 and 1578 to 1980. The annual ring for A.D. 1580 was missing from many trees at various sites in the study area.

The first half of the reconstruction is characterized by more persistent periods of high flow and low flow than the gaged record or the more recent reconstruction (Figure 5). In several of these periods, reconstructed six-year means are anomalous for perhaps half a century at a time. Examples are the high flows ending A.D. 940, and low flows ending near A.D. 1175 and A.D. 1400 (Figure 5). The transition from high to low flow near A.D. 1350 is particularly interesting because other paleoclimatic evidence supports an abrupt switch from extreme drought to very wet conditions than at more southerly latitudes in the Sierra Nevada and the neighboring White Mountains (Graumlich, 1993; Hughes and Graumlich, 1996; Hughes and Funkhouser, 1998; Stine, 1994). Such a latitudinal contrast is consistent with a reported north-south seesaw of precipitation in the region at decadal timescales, with a pivot point near 40°N (Dettinger *et al.*, 1998). The early centuries of our reconstruction are driven strongly by the tree-ring site in southern Oregon (Figure 2). The out-of-phase moisture anomalies between our reconstruction and the central and southern Sierra Nevada suggests a persistent southward shift of storm tracks to the south about A.D. 1350. Tree-ring chronologies from intermediate latitudes are needed, however, to corroborate such a shift.

Were droughts in the reconstruction more severe than any in the gaged record? The error term in regression causes reconstructed values to be compressed toward the calibration-period mean of flow. As a result, reconstructed flow anomalies are

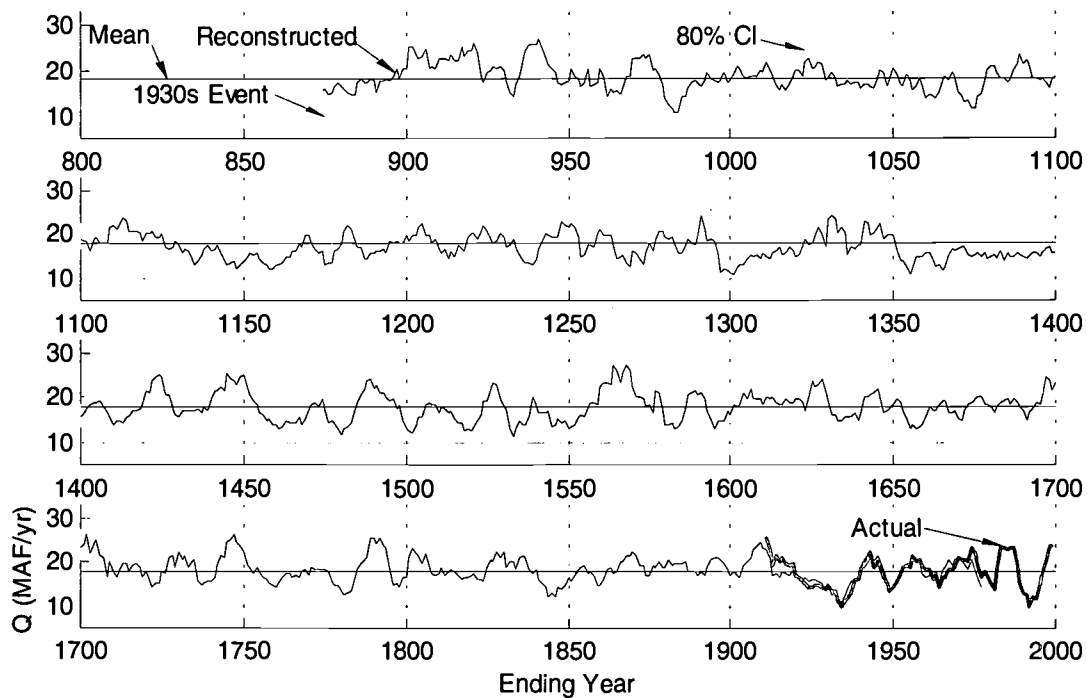


Figure 5. Six-Year Running Means of Gaged and Reconstructed Flow. Values are plotted at ending year of six-year period for the A.D. 869 to 1977 reconstruction and the 1906 to 1999 gaged record. Uncertainty in reconstructed values shown by 80 percent confidence interval derived by Monte Carlo analysis. Reference lines at long-term 1906 to 1999 mean (18.1 MAF) and record-low six-year mean of gaged flow.

TABLE 3. Lowest *n*-Year Moving Averages of Reconstructed and Actual Flow in Full-Length Reconstruction.*

Rank	1 Year	3 Year	6 Year	10 Year	20 Year	50 Year
1	1.52(1580)	6.96(1580)	10.55(983)	11.64(1301)	13.43(1311)	14.83(1399)
2	4.65(1059)	7.41(981)	10.79(984)	12.25(1302)	13.46(1158)	14.88(1396)
3	4.98(1532)	7.53(1581)	10.88(1934)	12.25(1304)	13.50(1159)	14.89(1400)
4	5.05(1529)	8.21(1778)	10.99(1355)	12.48(1303)	13.55(1312)	14.93(1397)
5	5.25(979)	8.68(1796)	11.00(1301)	12.91(1305)	13.58(1162)	14.95(1398)
1	5.12(1977)	8.87(1992)	9.79(1934)	12.27(1937)	13.54(1937)	16.38(1966)

*Table entries are averages of water-year flow (MAF) for *n*-year period ending with year in parentheses; rows 1-5 are five most severe reconstructed droughts and last row is most severe observed drought.

conservative, reconstructed highs and lows are less dramatic than those of the gaged record, and gaged and reconstructed extremes can be compared only in probabilistic terms. The 80 percent confidence bands have been applied above to identify years in which the probability exceeds 0.1 that flow in a reconstruction year was below the lowest gaged flow. Analysis of the empirical distributions of noise-added reconstructions can be extended to estimation of the probability that the actual flow in any reconstruction year or group of years was lower than the record-low of gaged flow. Nonexceedance probabilities derived from the full-length reconstruction for *n*-year means (*n* = 1, 3, 6,

10, and 20 years) are listed in the last column of Table 4. The most emphatic result is for the single year extreme of drought, A.D. 1580, which Hughes and Brown (1992) identified as one of the most extreme drought years in the San Joaquin drainage in the last 2,100 years. The critical value defined by the 1977 gaged low of 5.12 MAF has an empirically derived nonexceedance probability of 1.0 in reconstruction year A.D. 1580. In other words, the flow was almost certainly lower in A.D. 1580 than in 1977. The probability of 1.0 in this case arises from none of the 1,000 noise-added reconstructed values in A.D. 1580 exceeding 5.12 MAF. The probability is likewise high (*p* =

0.87) that flow in A.D. 1578 to 1580 was lower than the gaged three-year low that occurred in 1990 to 1992. Nonexceedance probabilities are at least 0.20 for other lengths of averaging period in Table 4. It is therefore reasonable to conclude that the lowest n -year mean flows in the gaged record for averaging periods of $n = 1, 3, 6, 10,$ and 20 may well not be the extreme low flows in a long-term context.

TABLE 4. Monte Carlo Summary of Reconstructed Droughts.

N ^a	Period (A.D.)	Flow (MAF/yr) ^b		$p(q < q_c)^c$
		\hat{q}	q_c	
1	1580	1.52	(5.12)	1.00
3	1578 to 1580	6.96	(8.87)	0.87
6	978 to 983	10.55	(9.79)	0.20
10	1292 to 1301	11.64	(12.27)	0.58
20	292 to 1311	13.43	(13.54)	0.34

^aNumber of years in running-mean.

^bLowest running mean of reconstruction (\hat{q}) and gaged record (q_c).

^cProbability that flow in listed period was lower than lowest flow of the gaged record.

CONCLUDING REMARKS

This study extends information on flow of the Sacramento River to the millennial time scale, and illustrates how the error term in tree-ring reconstructions can be used for probabilistic inferences about hydrologic drought before the start of the gaged record. Regression statistics suggest that the annual flow reconstruction is reasonably accurate for its full length and is among the most accurate dendrohydrologic reconstructions ever obtained for the period after A.D. 1630. The reconstruction supports use of the 1930s as a design period for extreme drought with duration of perhaps six to ten years. The gaged record appears to be less representative of extreme droughts of longer and shorter duration. Because of the buffering effect of storage reservoirs, the longer-duration droughts are perhaps of greater importance. Persistent high or low flows over several decades characterize the reconstruction before A.D. 1400. Such persistent flow anomalies, should they occur today, would challenge water-supply management for the basin. We emphasize, however, that the longest reconstructed droughts occurred in the earlier and least accurate part of the reconstruction.

In reconstructing by subperiods, we acknowledge the time-dependent quality of the dendrohydrologic

information for the Sacramento Basin. The respectably high regression R^2 for the earlier subperiods attests to the high spatial coherence of moisture anomalies, in the region during the 1906 to 1977 calibration period. The higher the spatial coherence of the moisture anomalies the less important the voids in the sampling network over the basin. But we cannot dismiss the possibility that the dominant spatial modes of moisture variation over the Sacramento Basin were different in the distant past than in the period used to calibrate the reconstruction models. For this reason the pre-1630 reconstruction, despite its impressive statistics, must be regarded as tentative, and the extended multi-decadal departures of flow inferred for this river system from the pre-1630 reconstruction must be corroborated with more tree-ring data from important runoff-producing regions. Millennial-length tree-ring data collected from the headwaters of American and Yuba Rivers in 1999 will eventually contribute to this effort, and possibly allow reconstruction of flow by subbasin within the Sacramento watershed.

ACKNOWLEDGMENTS

This work was supported by funding from the California Department of Water Resources and the NOAA Paleoclimatology Program (Awards NA 86GP0454 and ATM-9986074). We thank the contributors to the International Tree-Ring Data Bank, IGBP PAGES/World Data Center for Paleoclimatology, NOAA/NGDC Paleoclimatology Program, Boulder, Colorado, USA, for use of their data (see Appendix), and David Stahle for reading over the manuscript.

LITERATURE CITED

- California Department of Water Resources, 2000. March 16, WSIHIST. Available at <http://cdec.water.ca.gov/cgi-progs/ioidir/WSIHIST>, accessed July 13, 2000.
- Cleaveland, M. K. and D. W. Stahle, 1989. Tree Ring Analysis of Surplus and Deficit Runoff in the White River, Arkansas. *Water Resources Research* 25(6): 1391-1401.
- Conover, W., 1980. *Practical Nonparametric Statistics* (Second Edition). John Wiley and Sons, New York, New York.
- Cook, E. R., K. Briffa, and P. D. Jones, 1994. Spatial Regression Methods In Dendroclimatology: A Review and Comparison of Two Techniques. *International Journal of Climatology* 14:379-402.
- Cook, E. R. and G. C. Jacoby, 1983. Potomac River Streamflow Since 1730 as Reconstructed by Tree Rings. *J. Clim. Appl. Meteorology* 22:1659-1672.
- Crippen, J.R., 1986. California: Surface-Water Resources. In: *National Water Summary 1985 - Hydrologic Events and Surface-Water Resources*, U.S. Geological Survey Water-Supply Paper 2300, D. W. Moody, E. B. Chase, and D. A. Aronson (Compilers). U.S. Government Printing Office, Washington, D.C., pp. 157-166.

- Dettinger, M. D., D. R. Cayan, H. F. Diaz, and D. M. Meko, 1998. North-South Precipitation Patterns in Western North America on Interannual-to-Decadal Timescales. *J. of Climate* 11:3095-3111.
- Draper, N. R. and H. Smith, 1981. *Applied Regression Analysis* (Second Edition). John Wiley and Sons, Inc., 709 pp.
- Earle, C. J. and H. C. Fritts, 1986. Reconstructing Riverflow in the Sacramento Basin Since 1560. Report prepared for California Department of Water Resources under Agreement No. DWR B-55395.
- Fritts, H. C., 1976. *Tree rings and Climate*. Academic Press, London, U.K., 567 pp.
- Gordon, G., 1982. Verification of Dendroclimatic Reconstructions. *In: Climate from Tree Rings*, M. K. Hughes *et al.* (Editors). Cambridge University Press, Cambridge, U.K., pp. 58-61.
- Graumlich, L., 1993. A 1000-Year Record of Temperature and Precipitation in the Sierra Nevada. *Quaternary Research* 39:249-255.
- Graybill, D. A. and G. Funkhouser 2000. Dendroclimatic Reconstructions During the Past Millennium in the Southern Sierra Nevada and Owens Valley, California *In: Southern California Climate: Trends and Extremes of the Past 2000 Years*, R. Lavenberg (Editor). Natural History Museum of Los Angeles County, Los Angeles, California.
- Holmes, R. L., R. K. Adams, and H. C. Fritts, 1986. Tree-Ring Chronologies of Western North America: California, Eastern Oregon and Northern Great Basin with Procedures Used in the Chronology Development Work Including Users' Manuals for Computer Programs COFECHA and ARSTAN. Laboratory of Tree-Ring Research, University of Arizona, Tucson, Arizona.
- Hughes, M. K. and P. M. Brown, 1992. Drought Frequency in Central California Since 101 B.C. Recorded in Giant Sequoia Tree Rings. *Climate Dynamics* 6:161-7.
- Hughes, M. K., and G. Funkhouser 1998. Extremes of Moisture Availability Reconstructed From Tree Rings for Recent Millennia in the Great Basin of Western North America. *In: The Impacts of Climate Variability on Forests*, M. Innes and J. L. Beniston (Editors). Springer-Verlag, Berlin, Germany, pp 99-107.
- Hughes M. K. and L. J. Graumlich, 1996. Multimillennial Dendroclimatic Records From Western North America. *In: Climatic Variations and Forcing Mechanisms of the Last 2000 Years*, R. S. Bradley, P. D. Jones, and J. Jouzel (Editors). Springer Verlag, Berlin, Germany, pp. 109-24.
- Hughes, M. K., R. Touchan, and P. Brown 1996. A Multimillennial Network of Giant Sequoia Chronologies for Dendroclimatology. *In: Tree Rings, Environment and Humanity, Proceedings of the International Conference*, Dean, J., D. Meko and T. Swetnam (Editors). Radiocarbon, Tucson, Arizona, pp. 225-34.
- Jones, P. D. and M. Hulme, 1996. Calculating Regional Climatic Time Series for Temperature and Precipitation: Methods and Illustrations. *International J. of Climatology* 16:361-377.
- Mardia, K., J. Kent, and J. Bibby, 1979. *Multivariate Analysis*. Academic Press, 518 pp.
- Meko, D. M. and D. A. Graybill, 1995. Tree-Ring Reconstruction of Upper Gila River Discharge. *Water Resources Bulletin* 31(4):605-616.
- Michaelsen, J., 1987. Cross-Validation in Statistical Climate Forecast Models. *J. of Climate and Applied Meteorology* 26:1589-1600.
- NCDC, 2000. NCDC: Get/View On Line Climate Data. Available at <http://www.ncdc.noaa.gov/ol/climate/climatedata.html#MONTHLY>, accessed July 27, 2000.
- NGDC, 2000. Directory of /paleo/treering/chronologies/asciifiles. Available at <ftp://ftp.ngdc.noaa.gov/paleo/treering/chronologies/asciifiles>, accessed July 18, 2000.
- Rencher, A. C. and F. C. Pun, 1980. Inflation of R^2 in Best Subset Regression. *Technometrics* 22(1):49-53.
- Smith, L. P. and C. W. Stockton, 1981. Reconstructed Streamflow for the Salt and Verde Rivers From Tree-Ring Data. *Water Resources Bulletin* 17(6):939-947.
- Stine, S., 1994. Extreme and Persistent Drought in California and Patagonia During Mediaeval Time. *Nature* 369:546-549.
- Touchan, R. and D. M. Meko, 1999. A 396 Year Reconstruction of Precipitation in Southern Jordan. *Journal of the American Water Resources Association* 35(1):49-59.
- Weisberg, S., 1985. *Applied Linear Regression* (Second Edition). John Wiley and Sons, New York, New York, 324 pp.

APPENDIX – TREE-RING SITE INFORMATION.

Na	Site Name ^b		Spec ^c	Location ^d			Se	D ^f
				Lat.	Long.	El(m)		
1	LEMON CANYON	(ca064)	PIJE	39.57	-120.25	1859	0.12	1
2	DALTON RESERVOIR	(ca065)	PIPO	41.62	-120.70	1531	0.31	1
3	ANTELOPE LAKE	(ca066)	PIJE	40.15	-120.60	1480	0.15	1
4	ANTELOPE LAKE	(ca067)	PIPO	40.15	-120.60	1480	0.25	1
5	FELKNER RIDGE	(ca070)	PILA	39.50	-122.67	1494	0.17	1
6	HAGER BASIN RESE	(ca073)	JUOC	41.77	-120.75	1524	0.23	1
7	KAISER PASS	(ca087)	JUOC	37.28	-119.08	2731	0.34	1
8	BRYANT CREEK	(ca091)	PIMO	38.75	-119.67	2073	0.14	2
9	KENNEDY MEADOWS	(ca514)	PIJE	36.03	-118.18	2024	0.33	1
10	FLOWER LAKE	(ca528)	PIBA	36.77	-118.37	3291	0.25	3
11+	TIMBER GAP UPPER	(ca529)	PIBA	36.45	-118.60	3261	0.21	3
12	ONION VALLEY	(ca531)	PIBA	36.77	-118.35	2865	0.22	3
13	TIMBER GAP LOWER	(ca532)	PIBA	36.45	-118.62	3017	0.31	3
14+	CAMPITO MOUNTAIN	(ca533)	PILO	37.50	-118.22	3400	0.11	3
15*	METHUSELAH WALK	(ca535)	PILO	37.43	-118.17	2805	0.14	4
16	LONE LAKE	(ca556)	PICO	37.17	-118.47	2850	0.26	5
17	YOSEMITE PARK E	(ca560)	PICO	37.80	-119.25	3000	0.14	5
18	JACKSON MOUNTAIN	(nv060)	JUOC	41.30	-118.43	2097	0.31	1
19	CALAMITY CREEK	(or009)	JUOC	43.98	-118.80	1464	0.26	1
20	HORSE RIDGE	S (or012)	JUOC	43.97	-121.07	1146	0.43	1
21	LITTLE JUNIPER	M (or018)	JUOC	43.13	-119.87	1596	0.39	1
22	STEENS MOUNTAIN	(or021)	JUOC	42.67	-118.92	1656	0.18	1
23	CRATER LAKE NE-M	(or042)	TSME	42.97	-122.17	2200	0.29	5
24	BLACK CREEK	(blackck)	PIPO	37.25	-119.27	1798	0.17	1
25	LOST FOREST	(lostfor)	PIPO	43.37	-120.30	1374	0.39	1
26	AMERICAN RIVER	(amrcaqds)	QUDO	38.75	-121.10	185	0.37	6
27	MT DIABLO	(diacaqls)	QULO	37.87	-121.95	1000	0.59	6
28	EEL RIVER	(eelcaqds)	QUDO	39.82	-123.07	650	0.28	6
29	PINNACLES NATION	(pincaqds)	QUDO	36.47	-121.18	350	0.60	6
30	PACHECO PASS STA	(pppcaqds)	QUDO	37.05	-121.17	396	0.54	6
31	TUOLUMNE GROVE	(tuolumn)	SEGI	37.77	119.80	1707	0.15	7
32*	CAMP SIX	(campsix)	SEGI	36.77	-118.82	2038	0.29	8
33*	GIANT FOREST	(giantfor)	SEGI	36.55	-118.75	2042	0.13	8
34	EAST FORK	(eastfork)	SEGI	36.45	-118.67	1935	0.31	7
35*	CALAVERAS COUNTY	(calavers)	SEGI	38.27	-120.30	900	0.22	9
36*	FREDERICK BUTTE	(frbstd)	JUOC	43.58	-120.45	1494	0.51	10

^aSite number; sites in model T869 model marked by '*'; additional sites available for model T1100 model marked by '+'; all 36 sites in A.D. 1630 model.

^bSite name with name of chronology computer file in parentheses; files whose names start with two-letter state code downloaded from International Tree-Ring Data Bank.

^cSpecies code as used in International Tree-Ring Data Bank.

^dDecimal degrees latitude and longitude; elevation.

^eStrength of local precipitation signal in the tree-ring chronology, as measured by R^2 from multiple linear regression of chronology on water-year-total precipitation interpolated from station data to tree-ring site location.

^fData references: 1 - Holmes *et al.*, 1986; 2 - C. W. Stockton; 3 - D. A. Graybill; 4 - D. A. Graybill and V. C. LaMarche, Jr.; 5 - K. Briffa and F. H. Schweingruber; 6 - M. Therrell and D. Stahle; 7 - Hughes *et al.*, 1996; 8 - Hughes and Brown, 1992; 9 - C. Baisan and T. Swetnam; 10 - D. Meko and C. Baisan. Updated collection of site in Holmes *et al.*, 1986.